TMT

ALTERNATE SITE:

OBSERVATORIO DEL ROQUE DE LOS MUCHACHOS

TECHNICAL REPORT:
TMT MID INFRARED SENSITIVITY ANALYSIS

July 2021

www.tmt.org

TMT Mid Infrared Sensitivity Analysis

1. Purpose of this report

This report provides supplementary information about the TMT mid infrared (MIR) sensitivity analyses at ORM and Maunakea presented in the ORM Site Description Document (OSDD). It addresses comments raised during and after the 2020 site webinars on the comparative study of ORM/MK site conditions and the expected impact on TMT sensitivity throughout its operational wavelength range, based on which the analysis method was refined and additional validations of the TMT results were performed. We show that the MIR simulations are reliable and agree with independent simulations using a different radiative transfer model.[1]

In response to comments received in the webinars, the effect of telescope optics emissivity and the derivation of performance metrics relevant for anticipated science programs were reexamined and refined. This resulted in small differences to the values reported in the site webinars, but these are due to differences in the input assumptions, such as inclusion of the telescope optics emissivity or the zenith angle of observation, and not to changes to the underlying radiative transfer model. The updated results are reported here and are also incorporated into the OSDD.

Note that the goal of this document is only to

1. provide additional information on the method used to derive the results we presented in the OSDD and site webinars, and
2. to demonstrate the validity of the TMT MIR sensitivity model.

A comprehensive analysis of individual MIR science cases is very valuable in its own right and should be done at some point in the future, but it is beyond the scope of this report. We do, however, demonstrate that the tools used are suitable for such analyses.

This report is meant as a high-level summary. A journal article with the technical details of the simulations and results will also be prepared.

2. MIR sensitivity simulations

[1] We are grateful for feedback by and discussions with many MIR experts and interested parties, including but not limited to Philip Hinz, Andy Skemer, Chris Packham, Mitsuhiko Honda, Matt Richter, Gregory Herczeg and the TMT SAC.

2.1. RADIATIVE TRANSFER MODEL

The TMT MIR sensitivity simulations for ORM and Maunakea were done by the TMT operations development (DEOPS) team. The first and most important step of these simulations is a radiative transfer (RT) model that produces atmospheric transmission spectra for given ground temperature and precipitable water vapor (PWV) values. This model was developed by DEOPS team member Angel Otárola as part of his extensive work on the subject and has previously been validated against independent models several times, including ATRAN and an RT code developed by ESO.

Spectral line properties are taken from the HITRAN database (https://hitran.org/) and are updated whenever there is an update to HITRAN. Vertical profiles of temperature and PWV are derived from our own analysis of radiosonde data for the sites in question, using all-year median profile shapes adjusted in magnitude to produce the correct boundary conditions. The model includes the effects of pressure broadening, which causes saturated telluric emission lines to be 28% wider on average at ORM than at Maunakea.

The spectral resolution of the RT model is adjustable. The spectra shown in this report are results of simulations that cover the wavelength range from 1 to 25 µm simultaneously and are done with constant wavenumber spacing, resulting in the resolution being 40,000 at 1 µm, 8,000 at 5 µm and 2,000 at 20 µm. The exact resolution is not important for our purpose of validating the model and a general comparison of the sensitivities at ORM and Maunakea throughout the entire MIR wavelength range accessible to TMT (that is, covering L, M, N and Q bands). We note that studies of science cases involving resolved narrow lines are beyond the scope of this document, but the RT model can be run with higher resolution for a specific wavelength band if such studies should be desired in the future.

For a given ground temperature and PWV, the RT code saves atmospheric transmission spectra to a file. The spectra are then loaded and analyzed with a Matlab script. This script converts atmospheric transmissions to radiances, scales the spectra to the desired zenith angle and adds telescope and instrument backgrounds based on the ground temperature and the emissivity of the optics. In addition to the site comparison, the script can thus be used for sensitivity studies of the MIR performance with respect to these parameters (examples of which are shown in Section 3.2). It also produces the plots of the spectra and the relative sensitivities of the sites shown in the following sections of this report.

2.2. POINT SOURCE SENSITIVITY

The relative integration time between the sites is calculated using the point source sensitivity, PSS:

$$PSS \propto f_c D^4 \frac{S(X,\lambda)^2 t(X,\lambda)^2}{R(X,\lambda)}$$

Here, fc is the fraction of available nights, D is the telescope diameter, X is the airmass, S(X,λ) is the Strehl ratio of the observation, t(X,λ) is the atmospheric transmission and R(X,λ) is the background radiance of the atmosphere and the telescope optics. As the fraction of clear time and atmospheric turbulence conditions are very similar between ORM and Maunakea, in particular at MIR wavelengths, the relevant quantities for the comparison in this report are t(X,λ) and R(X,λ).

2.3. *INPUT PARAMETERS*

The input conditions for the simulations are as follows:

- Atmospheric transmission spectra from the radiative transfer model are available for 10%, 25% and 50% (median) conditions of nighttime temperature and PWV as shown in Table 1. The percentile values given in the table are all-year percentiles. See Section 3 for comments on seasonal variability.
- The radiative transfer model produces atmospheric transmission spectra at zenith, which can then be scaled to any zenith angle desired. The results validation is done for observing at zenith, with a sensitivity study as a function of zenith angle shown in Section 3.2. Results for different atmospheric conditions and a zenith angle of 30° are given in the appendix.
- For the results validation, optics emissivity is set to 11%, which includes 6% for the warm optics (1.5% for each of M1, M2, M3 and the entrance window to a cooled AO system) and 5% for other effects such as the M2 spiders, segment gaps, etc. This is a very optimistic estimate of the emissivity (applying only in the case of newly coated and absolutely clean optics) and thus an upper limit for the difference between ORM and MK. Using a larger emissivity reduces the difference between the two sites, as shown in the sensitivity study in Section 3.2 which also shows results for more realistic values in the ~20–30% range.

Table 1: Statistics of Precipitable Water Vapor and Nighttime Temperature for ORM and Maunakea.

Percentile	MK13N (4050m)		ORM (2250m)	
	PWV (mm)	Night Temp. (˚C)	PWV (mm)	Night Temp. (˚C)
5%	0.6	-2.3	1.0	-1.9
10%	0.8	-1.3	1.4	-0.8

25%	1.1	+0.4	2.2	+2.8
50%	1.9	+2.3	4.2	+8.1
75%	3.5	+3.9	7.0	+11.9

3. RESULTS

Results for 25% PWV and 25% temperature conditions and observation at zenith are shown in Figure 1. At any site, MIR observation with TMT will benefit from using the best conditions available. Most MIR observations at TMT will therefore be scheduled via an adaptive queue. As only ~10% of TMT observing time is expected to be spent on MIR observations and forecasts of PWV and temperature are comparatively easy over time scales of a few hours, a large fraction of these observations will happen in 25% or better conditions.[2]

The same plots for 10%, 25% and 50% conditions and observation at 30° zenith angle are shown in the appendix.

[2] Note that better than 25% temperature *and* 25% PWV conditions simultaneously happen somewhat less than 25% of the time, as PWV and temperature are not fully correlated. There is, however, some degree of correlation (low temperatures and low PWV happen predominantly in the winter). Thus, if scheduled correctly, a large fraction of the 10% of TMT time expected to be used for MIR observations will still happen in these or better conditions. See later in this section for a discussion of seasonal variability.

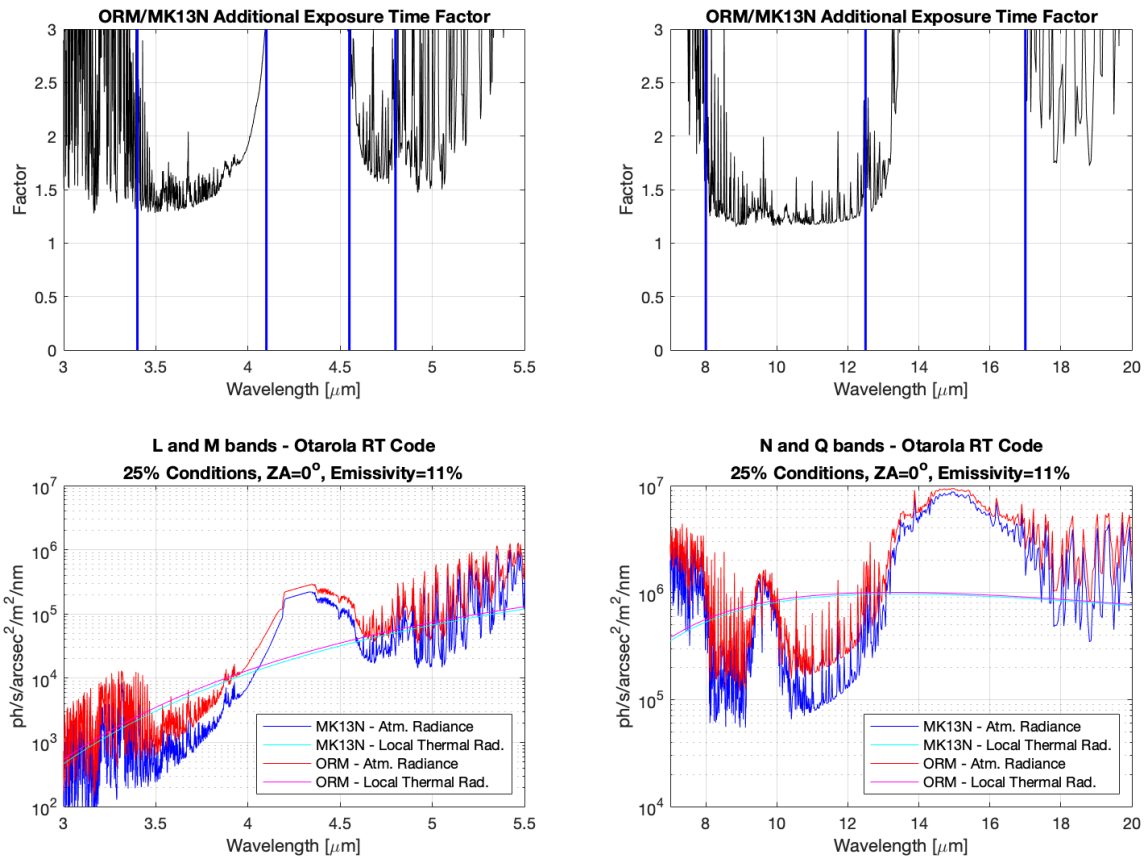

Figure 1: MIR sensitivities for 25% PWV, 25% nighttime temperature and observation at zenith at each site, split into L and M band on the left, and N and parts of Q band on the right. Blue is MK, red is ORM in the bottom plots. The top plots are the additional exposure time factor (ORM/MK). The vertical lines in the top plots indicate the limits of the L' (3.4–4.1 µm), M' (4.55–4.8 µm), N (8–12.5 µm) and Q (17–25 µm) bands. The resolution of these curves is reduced by a factor 5 for plotting purposes.

Many MIR observations concentrate on the transparent regions of the spectra in between atmospheric lines. For these regions, the lower envelop of the curves in the top plots of Figure 1 is the relevant metric for the comparison between the sites. For broadband imaging, an integral of the curves over the wavelength range of the filter provides the corresponding sensitivity.

Note that the spectra, as shown in the figure, cannot be used to quantify the site comparison of narrow atmospheric lines at the longer MIR wavelengths since their resolution is not sufficiently high for this purpose, as explained above. If such an analysis is desired in the future, the simulations can be rerun with a higher resolution for the wavelength range of interest.

Figure 1 shows results for all-year 25% conditions. Both PWV and temperature show seasonal variations that are stronger at ORM than at Maunakea. (See the OSDD for

detailed information on the seasonal variability of these parameters, as well as for other parameters such as usable time and seeing.) Thus, the relative sensitivities differ from those shown in the figure during different seasons. In brief, the difference between the sites is smaller in the winter, and larger in the summer. Again, a full analysis is beyond the scope of this report, but it can of course be done in order to analyze science cases for which observing during a specific season is critical.

3.1. COMPARISON WITH OTHER STUDIES

Following the site webinars, Philip Hinz at UCSC ran a similar analysis using his own code, an independent radiative transfer model and the same input conditions as those of Figure 1. Hinz's results are shown in Figure 2, demonstrating qualitative and quantitative agreement between the two models.

Direct comparisons of ORM/MK additional integration time between the Hinz and Otárola models are given in Figure 3 to Figure 5 for the different MIR wavelength bands. Figure 3 shows the results for N band. It can be seen that, in the transparent regions between absorption lines from 10 to 12.5 µm, the Hinz model shows an approximately 5% smaller increase of integration time than Otarola's model. Differences in other parts of N band are quantitatively different, but show the same good agreement between the two models. The figure also clearly shows that the TMT model does not underestimate the increase of integration time needed at ORM compared to other models.

Differences for the absorption lines appear to be larger in the figures, but this is due to the different spectral resolutions used for each of the two simulations. We note again that both models are internally run at higher resolution than what is plotted here. However, as they do not use the same resolution, differences between the data persist for narrow absorption lines even when the higher resolution data are plotted and the plots become so crowded that they are very hard to read in that case. The broader features, for example that at ~10.3 µm, show that absorption features are captured correctly.

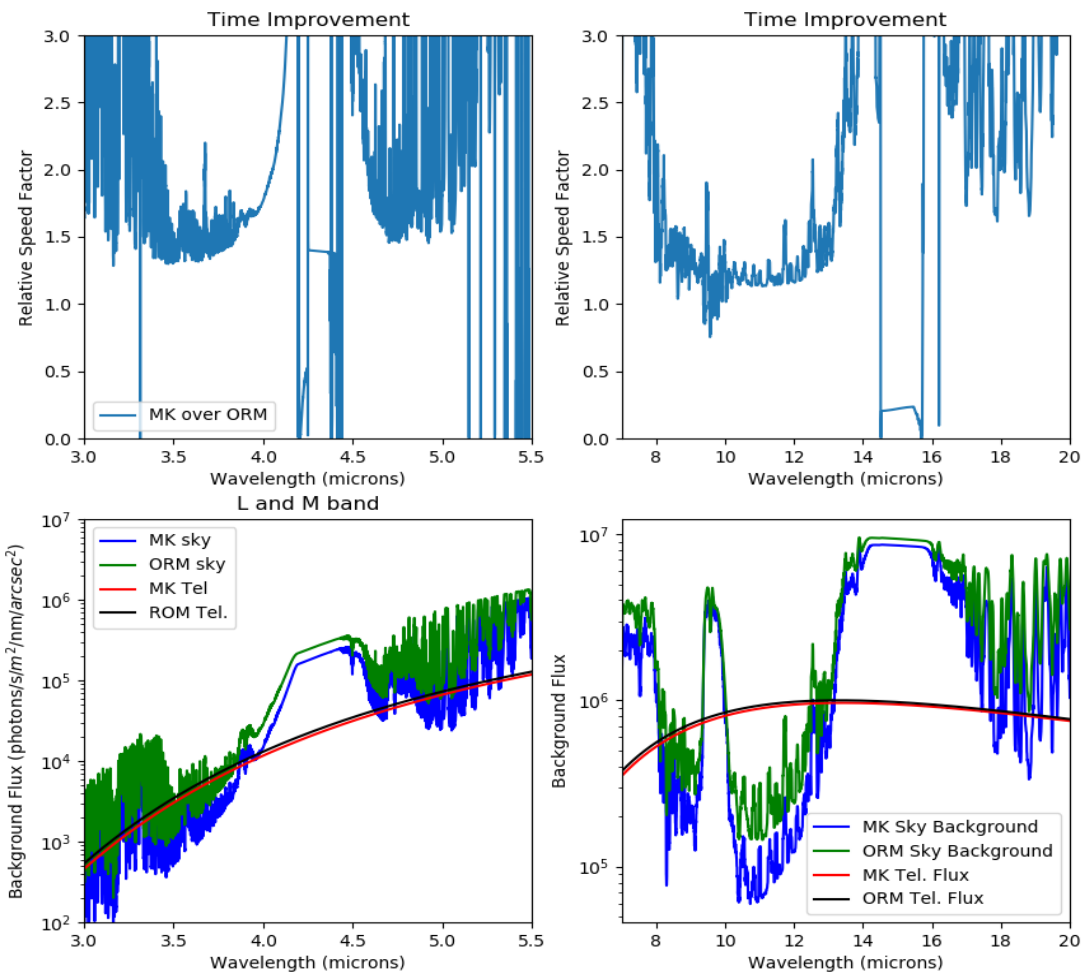

Figure 2: MIR sensitivities for the same conditions as in **Figure 1** calculated by Philip Hinz.

Figure 4 shows the same plot for L and M bands. The same good agreement is seen as for N band. One interesting feature here is the difference between the curves in the wing of L band, between 3.8 and 4.0 µm. This is due to slight differences in CO_2 abundances used in the two models.

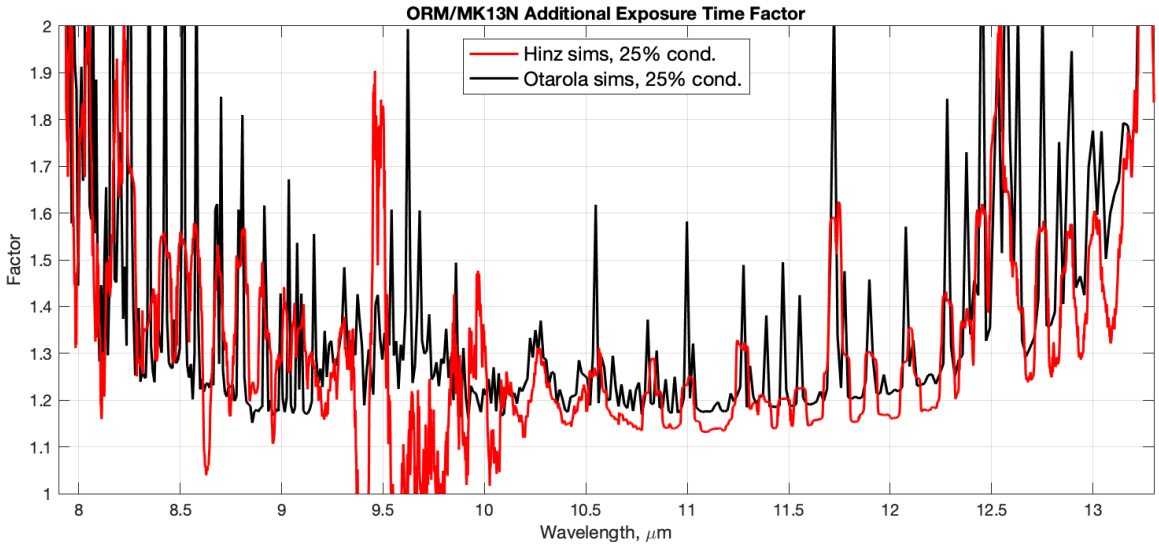

Figure 3: Comparison of the Hinz and Otárola simulations for N band.

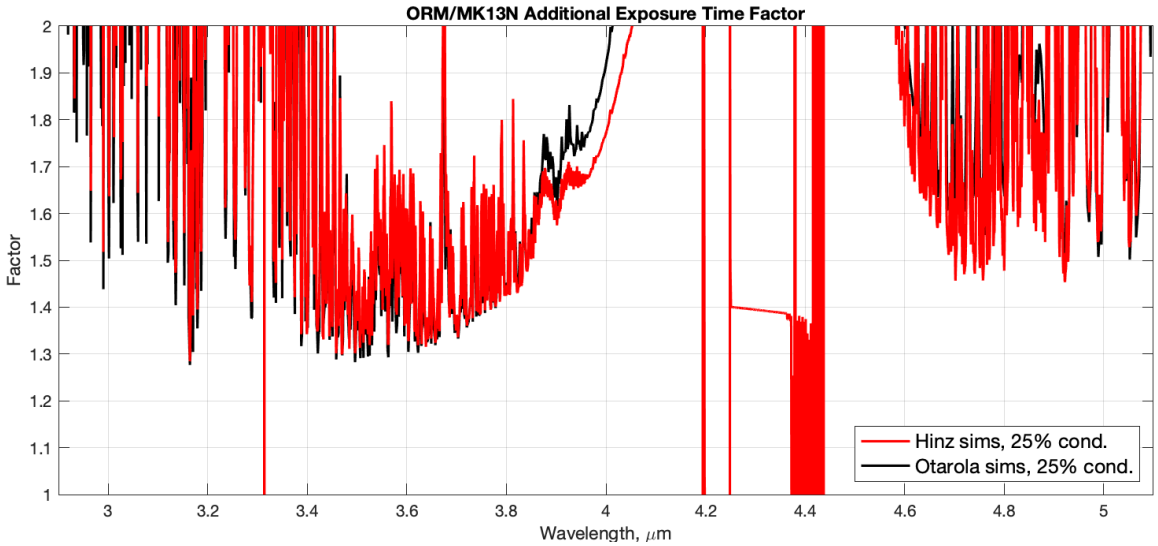

Figure 4: Comparison of the Hinz and Otárola simulations for L and M band.

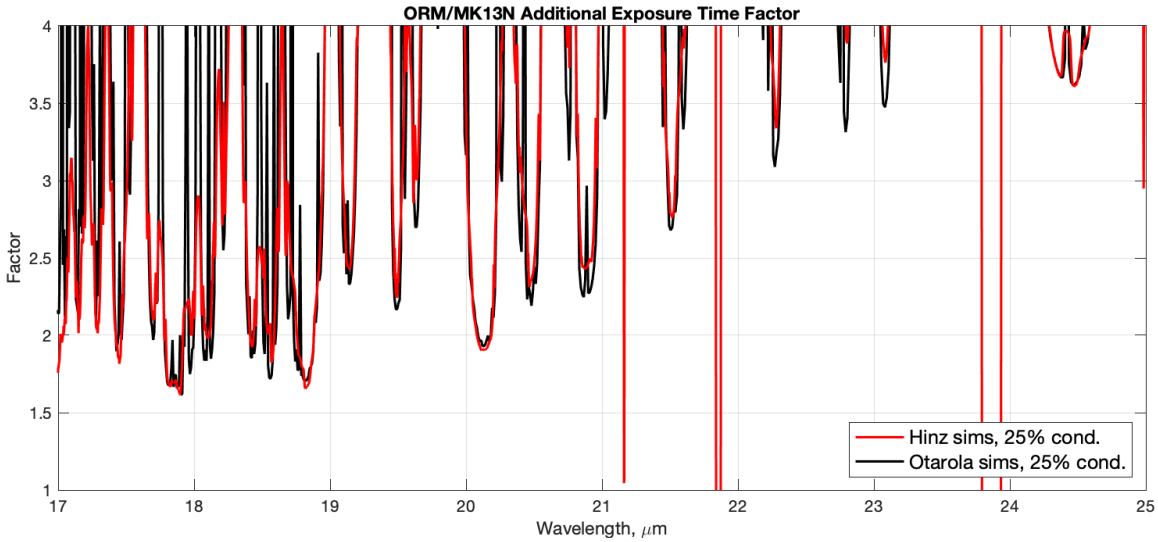

Figure 5: Comparison of the Hinz and Otárola simulations for Q band.

Finally, Figure 5 shows the same comparison for Q band. We can see very good agreement in the wider transparent regions, such as those at 17.8, 18.8 and 24.5 μm. The (somewhat) larger differences for the narrower lines are again due to the different resolutions of the two simulations.

3.2. ANALYSIS OF SENSITIVITY TO INPUT PARAMETERS

Figure 6 shows the dependence of the results on two of the main input parameters, zenith angle and optics emissivity, for N band using Otárola's RT model. The top plot shows the variation of the relative exposure times with zenith angle for a fixed emissivity of 11%. The figure shows that the variation of ORM/MK13N exposure times with increasing zenith angle does not scale directly with airmass, i.e. with atmospheric radiance. This is due to the important contribution from telescope background, even at this low emissivity.

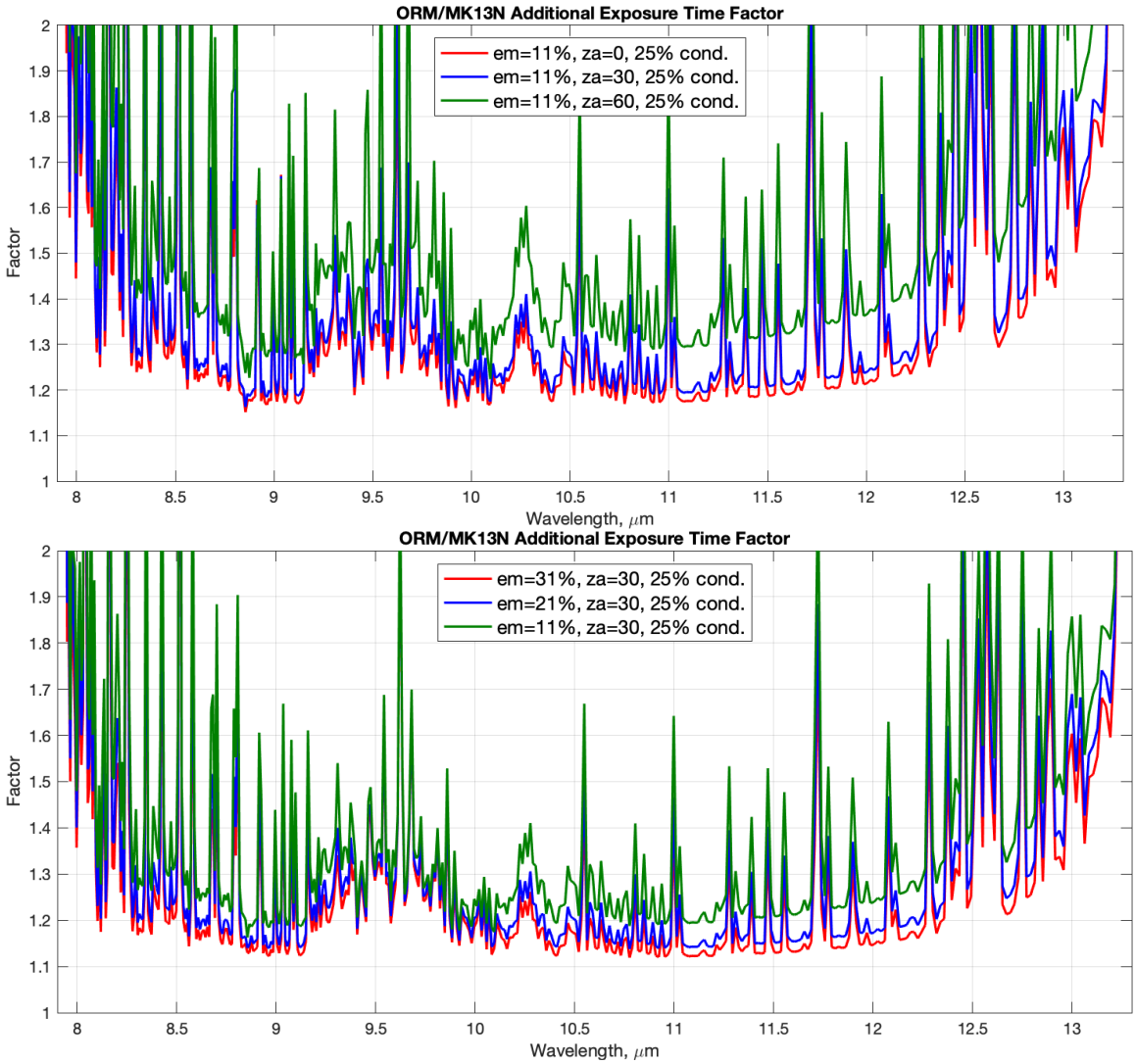

Figure 6: Sensitivity of the ORM/MK site comparison to zenith angle (top) and optics emissivity (bottom) for N band and 25% PWV and temperature conditions at each site.

The bottom plot shows the sensitivity curves in N band for optics emissivity of 11% (our base case that provides an upper limit to the difference between the two sites), and more realistic values of 21% and 31%. As expected, this plot shows that the sensitivity difference between the sites decreases with increasing optics emissivity.

3.3. METRICS

The previous version of the ORM Site Description Document and the site webinar presentations contain plots of scalar metrics of MIR site sensitivities. Based on the feedback we received, we now believe that such metrics are not very meaningful given the complexity of the spectra and the large variety of science cases. Depending on the

science case and its exact wavelength, or wavelength band, very different values are applicable. The best achievable ratios, when working in between atmospheric lines, can be read directly from the plots as the lower envelope of the relative integration time curves. More complex cases will have to be calculated on a case by case basis directly using the spectra. If anybody would like to do such analyses, we are happy to provide the radiative transfer model data.

4. SUMMARY AND CONCLUSIONS

This is a supplementary report to the ORM Site Description Document, presenting the background of the MIR sensitivity studies done for TMT and the comparison between the two sites, ORM and Maunakea. The original studies have been validated by comparison with an independent external model, the results of which are also shown. We find that the MIR sensitivity studies used for the analyses by the TMT team are robust and produce equivalent results to other models used for generating atmospheric transmission spectra. We explain the assumptions made for the MIR sensitivity studies and investigate how the results depend on input assumptions of observing angle and emissivity of the telescope optics. We show that realistic levels of telescope optics emissivity reduce the relative sensitivity difference between sites, and that the model used is suitable for more detailed analyses of specific MIR science cases.

5. APPENDIX – ADDITIONAL RESULTS

Figures Figure 7 to Figure 9 contain the same information as Figure 1, but for 10%, 25% and 50% conditions and observation at 30° zenith angle. Figures Figure 10 and Figure 11 show the sensitivity to zenith angle and optics emissivity (same as Figure 6) for L, M and Q bands.

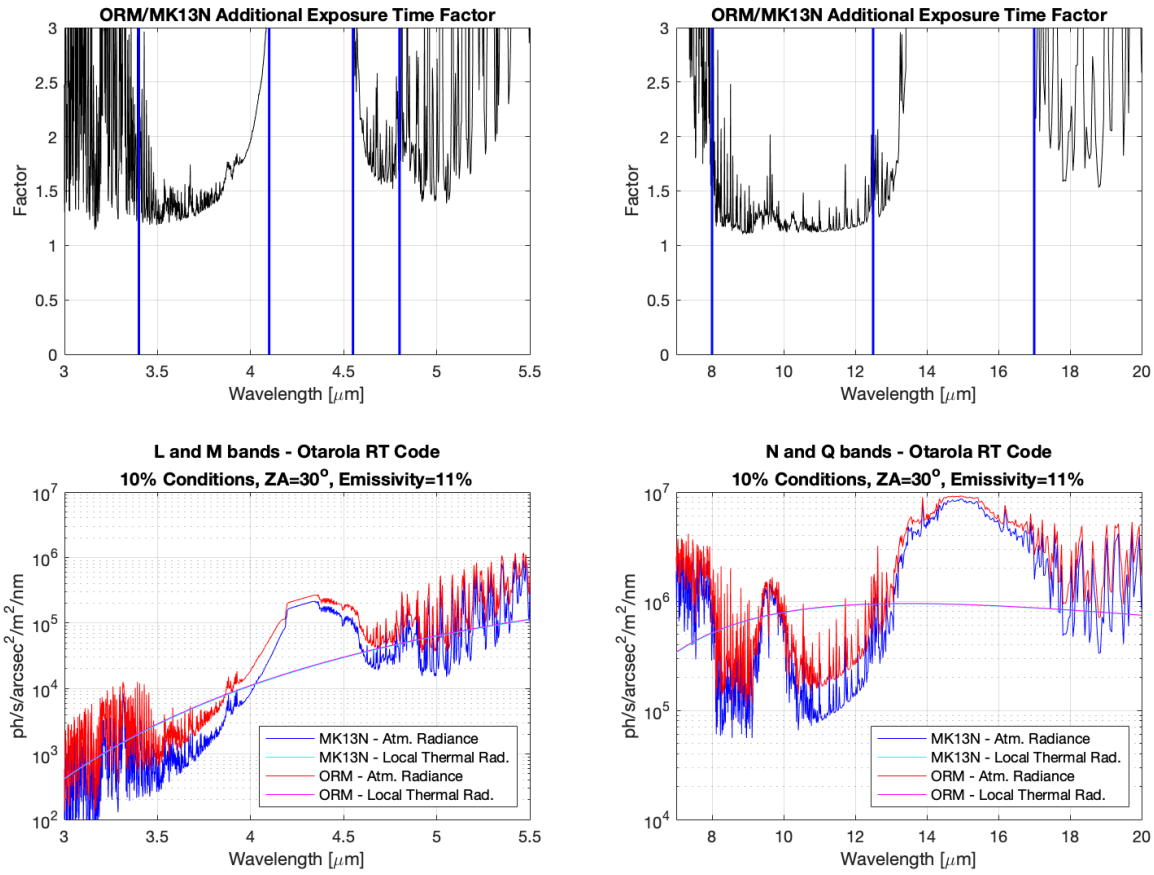

Figure 7: Same as **Figure 1** for 10% PWV, 10% nighttime temperature and observation at 30° zenith angle.

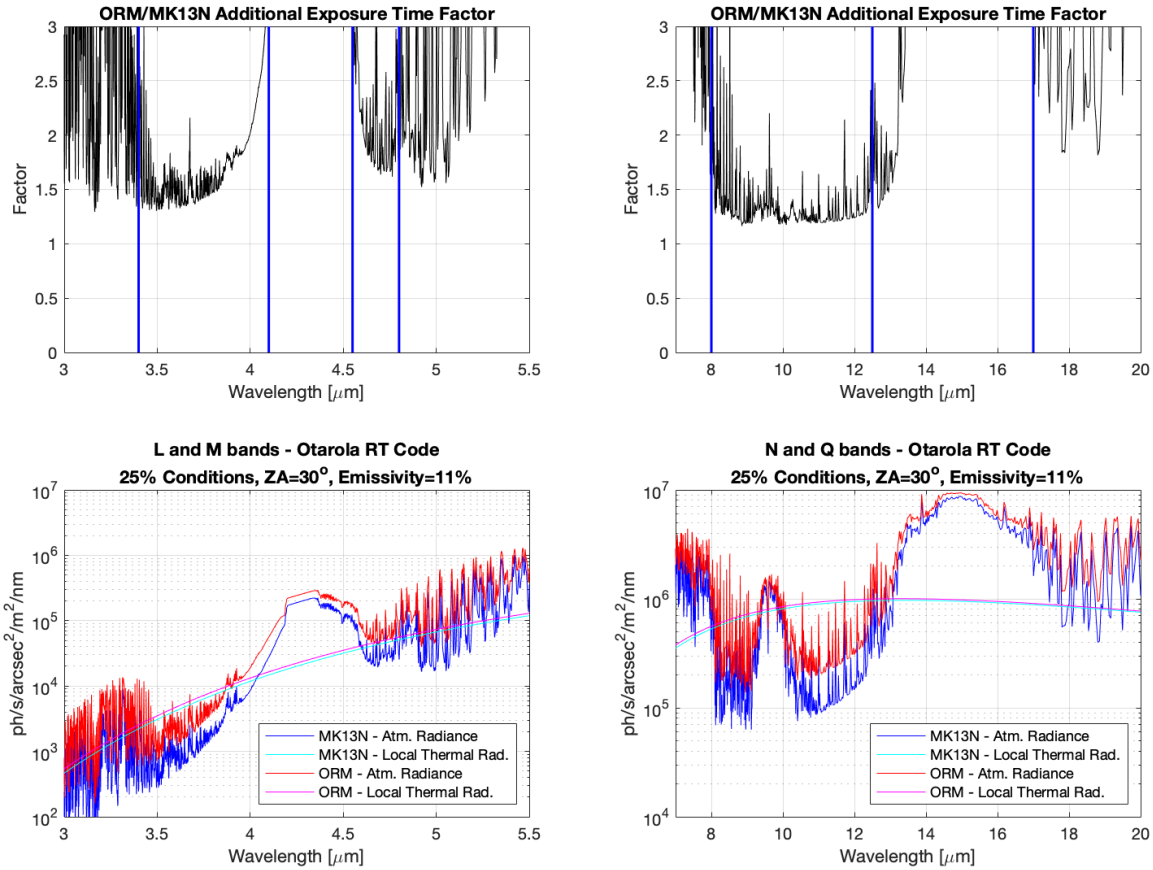

Figure 8: Same as **Figure 1** for 25% PWV, 25% nighttime temperature and observation at 30° zenith angle.

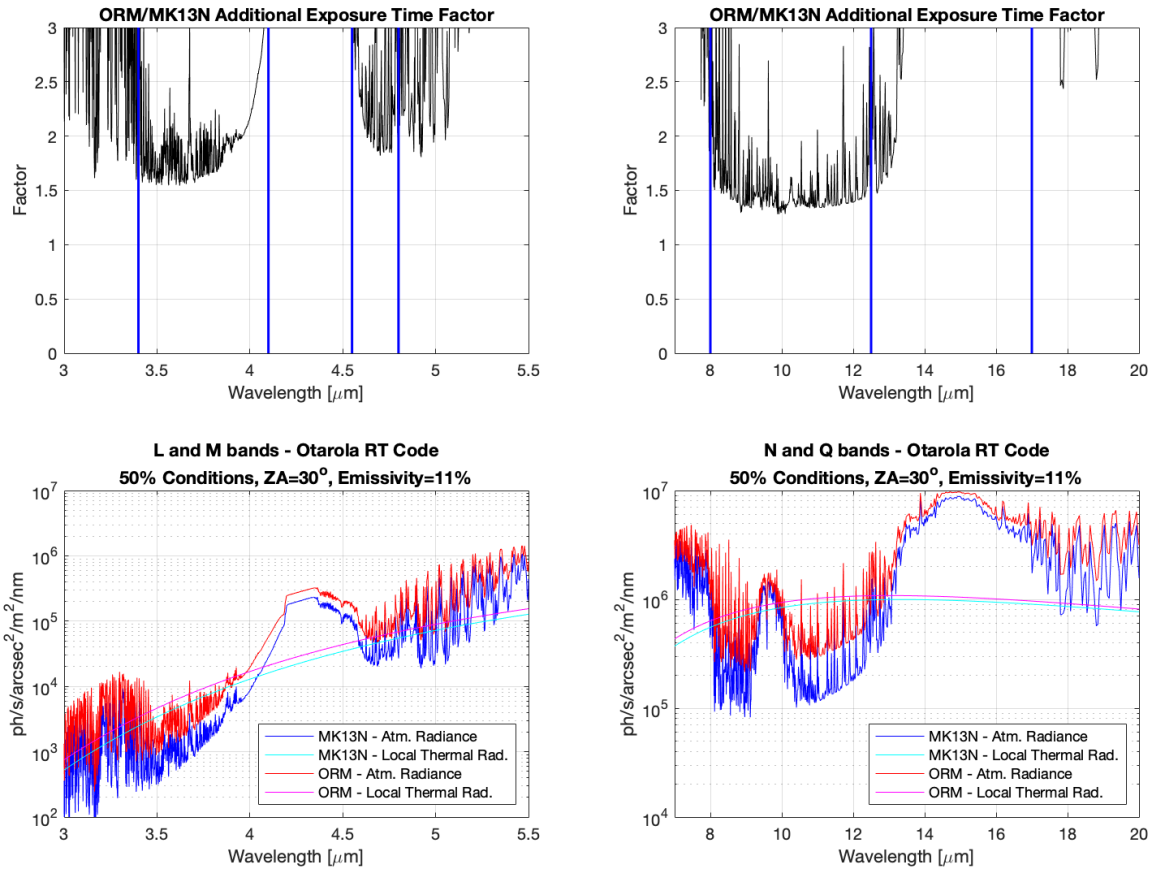

Figure 9: Same as **Figure 1** for 50% PWV, 50% nighttime temperature and observation at 30° zenith angle.

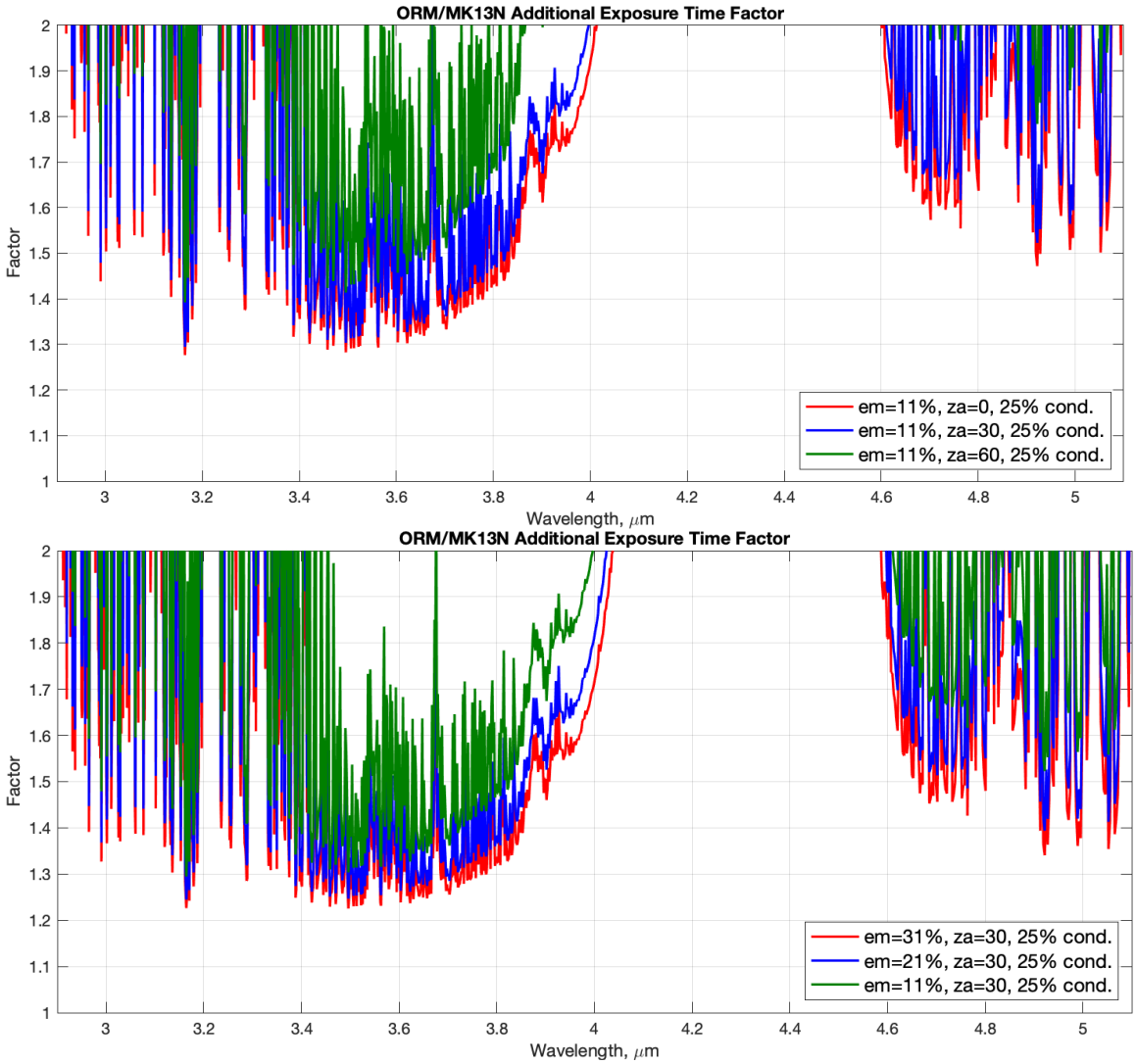

Figure 10: Sensitivity of the ORM/MK site comparison to zenith angle (top) and optics emissivity (bottom) for L and M bands and 25% PWV and temperature conditions at each site.

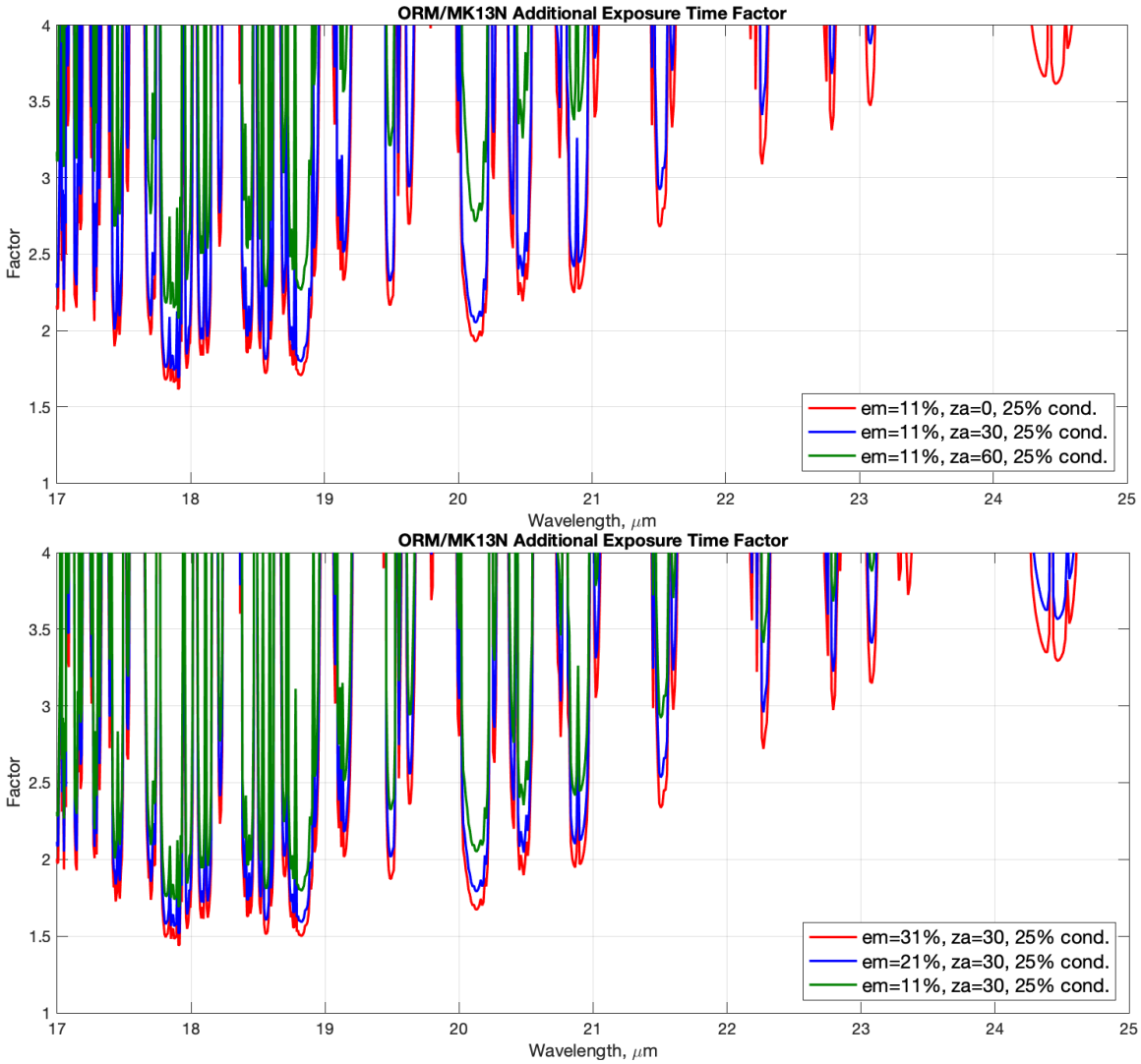

Figure 11: Sensitivity of the ORM/MK site comparison to zenith angle (top) and optics emissivity (bottom) for Q band and 25% PWV and temperature conditions at each site.